

A NEW FRAMEWORK FOR EUCLIDEAN SUMMARY STATISTICS IN THE NEURAL SPIKE TRAIN SPACE

BY SERGIUSZ WESOŁOWSKI, ROBERT J. CONTRERAS AND WEI WU

Florida State University

Statistical analysis and inference on spike trains is one of the central topics in the neural coding. It is of great interest to understand the underlying structure of given neural data. Based on the metric distances between spike trains, recent investigations have introduced the notion of an *average* or *prototype* spike train to characterize the template pattern in the neural activity. However, as those metrics lack certain Euclidean properties, the defined *averages* are nonunique, and do not share the conventional properties of a mean. In this article, we propose a new framework to define the mean spike train where we adopt a Euclidean-like metric from an L^p family. We demonstrate that this new mean spike train properly represents the average pattern in the conventional fashion, and can be effectively computed using a theoretically-proven convergent procedure. We compare this mean with other spike train averages and demonstrate its superiority. Furthermore, we apply the new framework in a recording from rodent geniculate ganglion, where background firing activity is a common issue for neural coding. We show that the proposed mean spike train can be utilized to remove the background noise and improve decoding performance.

1. Introduction. Neural spike trains are often called the language of the brain and are the focus of many investigations in computational neuroscience. Due to the stochastic nature of the spike discharge record, probabilistic and statistical methods have been extensively investigated to examine the underlying firing patterns [Rieke et al. (1999), Brown et al. (2002), Kass, Ventura and Brown (2005), Box, Hunter and Hunter (1978), Kass and Ventura (2001)]. However, these methods focus only on parametric representations at each given time and therefore can prove to be limited in data-driven problems in the space of spike trains.

Received June 2014; revised May 2015.

Key words and phrases. Spike train metrics, Euclidean summary statistics, mean spike train, neural coding, geniculate ganglion, background noise removal.

<p>This is an electronic reprint of the original article published by the Institute of Mathematical Statistics in <i>The Annals of Applied Statistics</i>, 2015, Vol. 9, No. 3, 1278–1297. This reprint differs from the original in pagination and typographic detail.</p>

Alternative approaches for analyzing spike train data are based on metrizing the spike train space. Over the past two decades, various methods have been developed to measure distances or dissimilarities between spike trains, for example, the distances in discrete state space, discrete time models [Lim and Capranica (1994), MacLeod, Bäcker and Laurent (1998), Rieke et al. (1999)], those in discrete state space, continuous time models [Victor and Purpura (1996), Aronov et al. (2003), Aronov and Victor (2004), Victor, Goldberg and Gardner (2007), Wu and Srivastava (2011)], those in continuous state space, continuous time models [van Rossum (2001), Houghton and Sen (2008), Houghton (2009)], and a number of others [Schreiber et al. (2003), Kreuz et al. (2007), Quian Quiroga, Kreuz and Grassberger (2002), Hunter and Milton (2003), Paiva, Park and Príncipe (2009)].

An ongoing pursuit of great interest in computational neuroscience is defining an average that can represent tendency of a set of spike trains. What follows is the problem of defining basic summary statistics reflecting the intuitive properties of the mean and the variance, which are crucial for further statistical inference methods. In particular, to make the first-order statistic, mean, convenient for constructing new framework and inference methods, it should satisfy the following properties:

1. The mean is uniquely defined in a certain framework.
2. The mean is still a spike train.
3. The mean represents the conventional intuition of average like in the Euclidean space.
4. The mean depends on exact spike times only, and is independent of the recording time period.
5. The mean can be computed efficiently.

Property 3 can be described as follows: given a set of N spike trains with each having K spikes, we denote these trains using vectors $\{(x_{i1}, \dots, x_{iK})\}_{i=1}^N$. Then the mean spike train is expected to resemble $\frac{1}{N} \sum_{i=1}^N (x_{i1}, \dots, x_{iK})$.

In Victor and Purpura (1997), the authors considered a “consensus” spike train, which is the centroid of a spike train set (under the Victor–Purpura metric). This idea was further generalized in Diez, Schoenberg and Woody (2012) to a “prototype” spike train which does not have to belong to the given set of spike trains, but its spike times are chosen from the set of all recorded spike times. Recently, a notion of an “average” based on kernel smoothing methods was introduced in Julienne and Houghton (2013). In Wu and Srivastava (2011, 2013), the authors proposed an elastic metric on inter-spike intervals to define a mean directly in the spike train space. However, none of these approaches satisfies the 5 desirable properties listed above, and therefore may result in limited use in practical applications.

In this article, we propose a new framework for defining the mean spike train. We adopt a recently developed metric related to an L^p family with

$p \geq 1$, which inherits desirable properties in the special case of $p = 2$ [Dubbs, Seiler and Magnasco (2010)]. This metric is a direct generalization of the Victor–Purpura metric, and we refer to it as a GVP (Generalized Victor–Purpura) metric. We will demonstrate that this new mean spike train satisfies all aforementioned 5 properties. In particular, the new framework is the only one (over all available methods) that has desirable Euclidean properties on the given spike times. Such properties are crucial for the definition of summary statistics such as the mean, variance, and covariance in the spike train space. In general, these 5 properties assure intuitiveness of the summary statistics, as well as efficiency in their estimation. In contrast, previous methods have issues such as nonuniqueness, dependence on model assumptions, or more complicated computations, and therefore do not result in the same level of performance (see the detailed comparison in Section 2.5).

One direct application of the mean spike train is in neural decoding in the rodent peripheral gustatory system [Wu et al. (2013)]. The neural data was recorded from single cells in geniculate ganglion, as the spiking activity in these neurons modulated with respect to different taste stimuli on the tongue. It is commonly known that spontaneous spiking activity can be observed even if only artificial saliva is applied. Thus, the neural response is actually a mixture of a background activity and a taste-stimulus activity. In this article we demonstrate using simulation as well as real data that the proposed new framework can be used to remove the background activity, which leads to improvement in decoding performance.

In Section 2 we define the new framework by introducing the mean spike train under the GVP metric, and provide an efficient algorithm to estimate it. In Section 3 we extend this framework by developing a statistical approach for noise removal and apply the method to the experimental data. We then discuss the merits of the new framework in Section 4. Finally, in the Appendix, we provide mathematical details on the convergence of the mean estimation algorithm.

2. New framework. Before we turn to describing the methods, it is necessary to set up a formal notation in the spike train space.

2.1. Notation. Assume S is a spike train with spike times $0 < s_1 < s_2 < \dots < s_M < T$, where $[0, T]$ denotes a recording time domain. We denote this spike train as

$$S = (s_j)_{j=1}^M = (s_1, s_2, \dots, s_M).$$

We define the space of all spike trains containing M spikes to be \mathcal{S}_M and the space of all spike trains to be $\mathcal{S} = \bigcup_{M=0}^{\infty} \mathcal{S}_M$. This can be equivalently described as a space of all bounded, finite, increasing sequences.

A time warping on the spike times (or inter-spike intervals) has been commonly used to measure distance between two spike trains [Victor and Purpura (1996), Dubbs, Seiler and Magnasco (2010), Wu and Srivastava (2011)]. Let Γ be the set of all time-warping functions, where a time warping is defined as an orientation-preserving diffeomorphism of the domain $[0, T]$. That; that is,

$$\Gamma = \{\gamma : [0, T] \rightarrow [0, T] \mid \gamma(0) = 0, \gamma(T) = T, 0 < \dot{\gamma}(t) < \infty\}.$$

It is easy to verify that Γ is a *group* with the operation being the composition of functions. By applying $\gamma \in \Gamma$ on a spike train $S = (s_j)_{j=1}^M$, one obtains a warped spike train $\gamma(S) = (\gamma(s_j))_{j=1}^M$.

2.2. GVP metric. In Dubbs, Seiler and Magnasco (2010), a new spike train metric was introduced with parameter $p \in [1, \infty)$. This metric is a direct generalization of the classical Victor–Purpura (VP) metric (VP is a special case when $p = 1$), and we refer to it as the Generalized Victor–Purpura (GVP) metric. In particular, when $p = 2$, this metric resembles a Euclidean L^2 distance.

Assume that $X = (x_i)_{i=1}^M$ and $Y = (y_j)_{j=1}^N$ are two spike trains in $[0, T]$. For $\lambda(> 0)$, the GVP metric between X and Y is given in the following form:

$$(1) \quad d_{\text{GVP}}[\lambda](X, Y) = \min_{\gamma \in \Gamma} \left(E_{\text{OR}}(X, \gamma(Y)) + \lambda^2 \sum_{\{i, j: x_i = \gamma(y_j)\}} (x_i - y_j)^2 \right)^{1/2},$$

where $E_{\text{OR}}(\cdot, \cdot)$ denotes the cardinality of the Exclusive OR (i.e., union minus intersection) of two sets. That is, $E_{\text{OR}}(X, \gamma(Y))$ measures the number of unmatched spike times between X and $\gamma(Y)$ and can be computed as

$$E_{\text{OR}}(X, \gamma(Y)) = M + N - 2 \sum_{i=1}^M \sum_{j=1}^N \mathbf{1}_{\{\gamma(y_j) = x_i\}},$$

where $\mathbf{1}_{\{\cdot\}}$ is an indicator function. The constant $\lambda(> 0)$ is the penalty coefficient. We emphasize that d_{GVP} is a proper metric, that is, it satisfies *positive definiteness*, *symmetry*, and *the triangle inequality*. It shares a lot of similarities with the classical L^2 norm.

Similarly to the result in Wu and Srivastava (2013), one can show that the optimal time warping between two spike trains $X = (x_i)_{i=1}^M$ and $Y = (y_j)_{j=1}^N$ must be a strictly increasing, piece-wise linear function, with nodes mapping from points in Y to points in X . Based on this fact, a dynamic programming algorithm was developed to compute the distance d_{GVP} with the computational cost of the order of $O(MN)$. Using the bipartite graph matching theory, another efficient algorithm was also developed to compute d_{GVP} in the cost of $O(MN)$ [Dubbs, Seiler and Magnasco (2010)].

2.3. *Definition of the summary statistics and their properties.* Conventional statistical inferences in the Euclidean space are based on basic quantities such as mean and variance. For statistical inferences in the spike train space, we can analogously use a Euclidean spike train metric to define these summary statistics as follows.

For a set of spike trains $S_1, S_2, \dots, S_K \in \mathcal{S}$ where the corresponding numbers of spikes are n_1, n_2, \dots, n_K (arbitrary nonnegative integers), respectively, we define their sample *mean* using the classical Karcher mean [Karcher (1977)] as follows:

$$(2) \quad S^* = \operatorname{argmin}_{S \in \mathcal{S}} \sum_{k=1}^K d_{\text{GVP}}[\lambda](S_k, S)^2.$$

When the mean spike train S^* is known, the associated (scalar) sample variance, σ^2 , can be defined in the following form:

$$(3) \quad \sigma^2 = \frac{1}{K-1} \sum_{k=1}^K d_{\text{GVP}}[\lambda](S_k, S^*)^2.$$

The computation of this variance is straightforward, and the main challenge is in computing the mean spike train for any $\lambda(> 0)$.

Before we move on to the computational methods for the summary statistics, we list several basic theoretical properties of the mean spike trains using the d_{GVP} metric. The proofs are omitted here to save space:

1. The optimal time warping between two spike trains must be a continuous, increasing, and piece-wise linear function between subsets of spike times in these two trains.

2. Let spike trains $X = (x_i)_{i=1}^M, Y = (y_i)_{i=1}^M \in \mathcal{S}_M$ be defined on $[0, T]$. If $\lambda^2 < 1/(MT^2)$, then

$$d_{\text{GVP}}[\lambda](X, Y) = \left(\lambda^2 \sum_{i=1}^M (x_i - y_i)^2 \right)^{1/2}.$$

3. Assume a set of spike trains $S_1, S_2, \dots, S_K \in \mathcal{S}$ with n_1, n_2, \dots, n_K spikes, respectively, and let $N_{\max} = \max(n_1, n_2, \dots, n_K)$. If $\lambda^2 < 1/(KN_{\max}T^2)$, then the number of spikes in the mean train is the *median* of $\{n_k\}_{k=1}^K$.

4. Let spike trains $S_1, \dots, S_K \in \mathcal{S}_M$. If $\lambda^2 < 1/(KMT^2)$, then the mean spike train has a conventional closed-form:

$$\frac{1}{K} \sum_{k=1}^K S_k.$$

2.4. *Computation of the mean spike train.* To compute the mean spike train S^* under the GVP metric, we need to estimate two unknowns: (1) the number of spikes n , and (2) the placements of these spikes in $[0, T]$. For a general value of $\lambda > 0$, neither the matching term nor the penalty term is dominant, and therefore we cannot identify the number of spikes in the mean before estimating their placements [Wu and Srivastava (2011)]. A key challenge is that we need to update the number of spikes in the algorithm. In this article, we propose a general algorithm to estimate the mean spike train. We initialize the number of spikes in the mean spike train equal to the maximum of $\{n_1, n_2, \dots, n_K\}$, and then adjust this number during the iterations. We present, here, how the Karcher mean in equation (2) can be efficiently computed using a convergent procedure.

2.4.1. *Algorithm.* Assume that we have a set of K spike trains, S_1, \dots, S_K with n_1, n_2, \dots, n_K spikes, respectively. Denote $S_k = (s_i^k)_{i=1}^{n_k}$ and $S = (s_i)_{i=1}^n$. Then the sum of squared distances in equation (2) is

$$(4) \quad \sum_{k=1}^K d_{\text{GVP}}[\lambda](S^k, S)^2 = \sum_{k=1}^K \min_{\gamma \in \Gamma} \left(E_{\text{OR}}[S^k, \gamma(S)] + \lambda^2 \sum_{\{i,j:s_i^k=\gamma(s_j)\}} (s_i^k - s_j)^2 \right).$$

We develop here an iterative procedure to minimize $\sum_{k=1}^K d_{\text{GVP}}[\lambda](S^k, S)^2$ (as a function of S) and estimate the optimal S^* . This new algorithm has four main steps in each iteration: Matching, Adjusting, Pruning, and Checking, and we refer to it as the MAPC algorithm. In particular, the Adjusting step corresponds to the Centering step in the MCP-algorithm in Wu and Srivastava (2013); in contrast to the nonlinear warping-based Centering-step, the Adjusting step utilizes the Euclidean property and updates the mean spike train in an efficient linear fashion. The Checking step is mainly used to avoid underestimating the number of spikes in the mean. This step adds one spike into the current mean and checks if such an addition results in a better mean (i.e., smaller mean squared distances). In contrast, such a problem is not addressed in the MCP algorithm.

Matching–Adjusting–Pruning–Checking (MAPC) Algorithm:

1. Let $n = \max\{n_1, n_2, \dots, n_K\}$. (Randomly) set initial times for the n spikes in $[0, T]$ to form an initial S .
2. *Matching step:* Use the dynamic programming procedure [Wu and Srivastava (2011)] to find the optimal matching γ^k from S to $S^k, k = 1, \dots, K$.

That is,

$$(5) \quad \gamma^k = \underset{\gamma \in \Gamma}{\operatorname{argmin}} \left(E_{\text{OR}}[S^k, \gamma(S)] + \lambda^2 \sum_{\{i,j: s_i^k = \gamma(s_j)\}} (s_i^k - s_j)^2 \right).$$

3. *Adjusting step:*

(a) For $k = 1, \dots, K, j = 1, \dots, n$, define

$$r_j^k = \begin{cases} s_i^k, & \text{if } \exists i \in \{1, \dots, n_k\}, \text{ s.t. } \gamma^k(s_j) = s_i^k, \\ s_j, & \text{otherwise.} \end{cases}$$

(b) Denote $R_k = (r_1^k, \dots, r_n^k), k = 1, \dots, K$. Then we update the mean spike train to be $\tilde{S} = \frac{1}{K} \sum_{i=1}^K R_i$.

4. *Pruning step:* Remove spikes from the proposed mean \tilde{S} that are matched less than $K/2$ times.

(a) For each $j = 1, \dots, n$, count the number of times s_j appears in $\{\gamma^k(S^k)\}_{k=1}^K$. That is, $h_j = \sum_{k=1}^K 1_{s_j \in \gamma^k(S^k)}$.

(b) Remove s_j from \tilde{S} if $h_j \leq K/2, j = 1, \dots, n$, and denote the updated mean spike train as \tilde{S}^* . Then

$$\tilde{S}^* = \{s_j \in \tilde{S} | h_j > K/2\}.$$

5. *Checking step:* To avoid being stuck in a local minimum, we check if an insertion or/and deletion of a specific spike can improve the mean estimation:

(a) Let \hat{S}^* be \tilde{S}^* except one spike with the minimal number of appearances (randomly chosen if there are multiple spikes at the minimum) in the Pruning step. Then, update the mean as

$$S^{**} = \begin{cases} \hat{S}^*, & \text{if } \sum_{k=1}^K d_{\text{GVP}}[\lambda](S^k, \hat{S}^*)^2 < \sum_{k=1}^K d_{\text{GVP}}[\lambda](S^k, \tilde{S}^*)^2, \\ \tilde{S}^*, & \text{otherwise.} \end{cases}$$

(b) Let \hat{S}^{**} be the current mean S^{**} with one spike inserted at random within $[0, T]$. Then update the mean as

$$S^{***} = \begin{cases} \hat{S}^{**}, & \text{if } \sum_{k=1}^K d_{\text{GVP}}[\lambda](S^k, \hat{S}^{**})^2 < \sum_{k=1}^K d_{\text{GVP}}[\lambda](S^k, S^{**})^2, \\ \tilde{S}^{**}, & \text{otherwise.} \end{cases}$$

6. *Mean update:* Let $S = S^{***}$ and n be the number of spikes in S .

7. If the sum of squared distances stabilizes over steps 2–6, then the mean spike train is the current estimate and we can stop the procedure. Otherwise, go back to step 2.

Denote the estimated mean in the m th iteration as $S^{(m)}$. One can show that the sum of squared distances (SSD), $\sum_{k=1}^K d_{\text{GVP}}[\lambda](S^k, S^{(m)})^2$, decreases iteratively as a function of m . As 0 is a natural lower bound, the SSD will always converge when m gets large. The detailed proof is given in the [Appendix](#). Note that this MAPC algorithm takes only linear computational order on the number of spike trains in the set. In practical applications, we find that this algorithm has great efficiency in reaching a reasonable convergence to a mean spike train.

In general, when the penalty coefficient λ gets large, the optimal time warping chooses to have fewer matchings between spikes to lower the warping cost. Some of the spikes in the mean will be removed during the iterations to minimize the SSD. In the extreme case, when λ is sufficiently large, any time warping would be discouraged (as that will result in a larger distance than simply the Exclusive OR operation). In this case, the mean spike train will be an empty train. This result indicates that in order to get a meaningful estimate of the mean spike train, the penalty coefficient λ should not take a very large value. In practical use, one may use a cross-validation to decide the optimal value of λ .

2.4.2. Illustration of the MAPC algorithm. To test the performance of the MAPC algorithm, we illustrate the mean estimation using 30 spike trains randomly generated from a homogeneous Poisson point process. Let the total time $T = 1$ (sec), the Poisson rate $\rho = 8$ (spikes/sec). The individual spike trains are shown in Figure 1A. The number of spikes in these trains varies

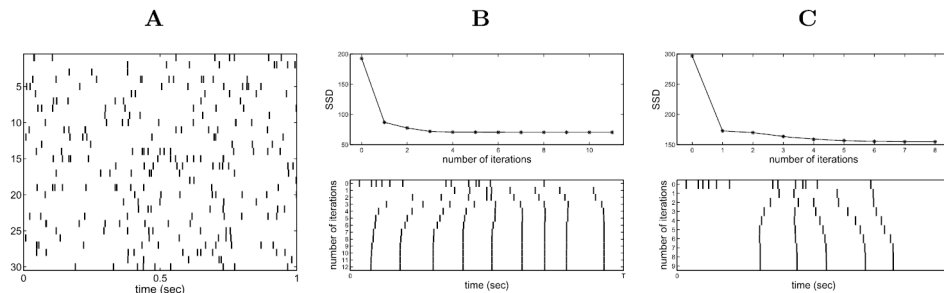


FIG. 1. A: 30 spike trains generated from a homogeneous Poisson process. Each vertical line indicates a spike. B: Estimation results when $\lambda^2 = 6$. Upper panel: The sum of squared distances (SSD) over all iterations. Lower panel: The estimated mean spike train over all iterations. The initial is the spike train on the top row (0), and the final estimate is the spike train on the bottom row (12th). C: Estimation result when $\lambda^2 = 60$.

from 3 to 13, with the median value of 9. Therefore, n , the number of spikes in the mean, is initialized to be 13 and we adopt randomly distributed 13 spikes in $[0, T]$ as the initial for the mean in each case. We let λ^2 vary between 6 and 60 to show the behavior for a small and a large warping penalty.

The result for the MAPC algorithm for $\lambda^2 = 6$ is shown in Figure 1B. The upper panel shows the evolution of the SSD in equation (2) versus the iteration index. We see that it takes only a few iterations for the SSD to decreasingly converge to a minimum. The estimated mean spike trains over iteration are shown in the lower panel. Apparent changes are observed in the first few (1 to 5) iterations, and then the process stabilizes. Note that the spikes in the mean train are approximately evenly spaced, which properly captures the homogeneous nature of the underlying process. We also note that the number of spikes in this mean spike train is 9, which equals the median of the numbers of spikes in the set.

The result for $\lambda^2 = 60$ is shown in Figure 1C. With a larger penalty, the optimal time warping between spike trains chooses to have fewer matchings between spikes to lower the warping cost. Some of the spikes in the mean are removed during the iteration. In this case, the convergent SSD is about 150, which is greater than the SSD when $\lambda^2 = 6$ (at about 80). Note that when λ is even larger, we expect fewer or even no spikes to appear in the estimated mean.

2.5. *Advantages over previous methods of averaging spike trains.* There have been multiple ideas of capturing the general trend in a set of spike trains, which include the “consensus” spike train [Victor and Purpura (1997)], the “prototype” spike train [Diez, Schoenberg and Woody (2012)], the “average” spike train [Julienne and Houghton (2013)], and the “mean” spike train [Wu and Srivastava (2011)]. However, none of those concepts satisfies all desirable 5 properties of a mean spike train listed in the Introduction section. We have summarized the most relevant differentiating features in Table 1. In the case of the “consensus” and “prototype” spike trains, one main problem lies in the nonuniqueness of the results in the spike train space, which arises directly from the underlying metric used (resembles Manhattan distance). If the estimated spiking times of those averages are restricted to spiking times in the sample sets, then the estimates can be unreliable, particularly when sample sizes are relatively small. The “average” design uses the van Rossum metric, which relies on kernel-smoothing of the spike trains. The estimation of the “average” is based on a greedy algorithm, but the accuracy and the kernel dependence of the method have not been carefully examined. In this article, we propose a new notion of a “mean” spike train based on the kernel-free GVP metric. The key advantages behind our design are the Euclidean properties of GVP distance and the subsequent Karcher mean definition [in

TABLE 1
Comparison of average of spike trains for different methods

Method	“mean” (proposed framework)	“consensus” Victor and Purpura (1997)	“prototype” Diez, Schoen- berg and Woody (2012)	“average” Julienne and Houghton (2013)	“mean” Wu and Srivastava (2011)
Metric used	GVP metric	Victor– Purpura metric	Victor– Purpura metric	van Rossum metric	Elastic metric
Properties (in Introduction) satisfied	1, 2, 3, 4, 5	2, 4, 5	2, 4, 5	1, 2, 4	1, 2, 5
Domain	Full spike train space	Given sample set	Given spike times set	Full spike train space	Full spike train space
Number of spikes, $\lambda^2 \ll 1$	Median of $\{n_1, \dots, n_N\}$	NA	NA	NA	median of $\{n_1, \dots, n_N\}$
Spike times if $n_1 = \dots = n_N$, $\lambda^2 \ll 1$	$c_j = \frac{1}{N} \sum_{k=1}^N s_{kj}$	Restricted to sample set	Restricted to sampled spike times	NA	ISI-based nonlinear form
Uniqueness in the full space	Almost surely	Nonunique	Nonunique	Not known	Almost surely

equation (2)]. The new framework satisfies all 5 desirable properties, which distinguishes it from others.

It is worth noting that, to the best of our knowledge, the GVP metric is one of only two spike train metrics that have Euclidean properties [the other one is the Elastic metric proposed in Wu and Srivastava (2011)]. However, the Elastic metric satisfies only 3 out of the 5 properties, and the GVP metric has two apparent advantages over it: first, the Elastic metric estimates the mean spike train explicitly depending on recording intervals. Such dependence may introduce an additional level of noise arising from experimental parameters, making the inference less reliable. In contrast, the mean spike train under the GVP metric relies only on exact spike times in the given data and is independent of recording intervals (Property 4). Second, the fact that the Elastic mean is estimated through the inter-spike intervals (ISI) makes it difficult to capture the intuition behind the result, whereas the GVP mean is estimated directly through spike times and resembles the intuition of the mean estimation (Property 3).

For illustrative purposes, we compare spike train “averages” of all methods using the 30 spike trains in Section 2.4.2, where the data is simulated under a homogeneous Poisson process. A natural expectation is that these averages should be *equi-distantly* spaced across the time domain. We adopt a simple

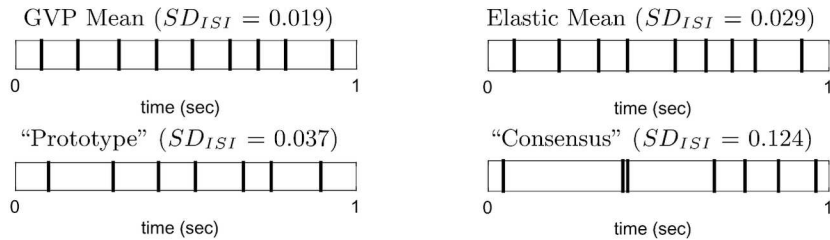


FIG. 2. *Averaged spike trains according to four different methods.*

measure for the equi-distant spacing—compute the standard deviation of the ISI in each train, denoted by SD_{ISI} . Basically, smaller SD_{ISI} values indicate more even spacing. In Figure 2, we show the averages estimated using the GVP mean, Elastic mean, “Prototype,” and “Consensus” methods. (In the GVP and Elastic methods, we let penalty coefficients be sufficiently small.) It is found that SD_{ISI} in the GVP mean is 0.019, the smallest over all four methods.

3. Application in noise removal. The notion of the mean spike train has a direct application in neural decoding. In this article we examine how the mean can be used to remove spontaneous activity in geniculate ganglion neurons and improve decoding performance.

3.1. Noise-removal method. Geniculate ganglion neurons exhibit spiking response to the chemical stimulus applied on the taste buds on the tongue. Such neuronal activity is commonly used in the neural coding in the peripheral gustatory system [Di Lorenzo, Chen and Victor (2009), Breza, Nikonov and Contreras (2010), Lawhern et al. (2011)]. We note that these neurons exhibit responses even if there is no stimulus applied or the stimulation is a control solution—artificial saliva. That is, the observed spike trains under the stimulation are likely to be a mixture of the spontaneous activity and responses to the taste stimuli. In the context of neural decoding, such spontaneous activity can be viewed as “background noise,” and a “de-noised” spiking activity is expected to better characterize the neural response with respect to the taste stimulus and result in better decoding performance.

Previous approaches to the noise-removal focus mainly on spike count across a time domain and do not have a temporal matching between spikes. In this paper, we propose a novel noise-removal procedure based on our new framework. In Figure 3 we describe the schematic idea of incorporating the noise removal in statistical inference. The procedure assumes that the observed data is a “sum” of isolated neuron responses and their spontaneous activity. To improve the neural decoding, we at first use the stimulus-free spike recordings to estimate the mean background noise with the MAPC

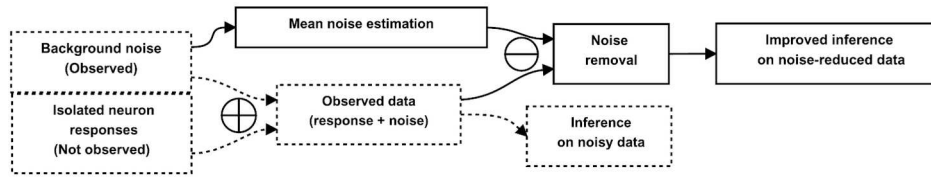


FIG. 3. Scheme differentiating the noise-removal approach from standard inference on spike train data. Dashed boxes indicate the components of standard inference framework, the solid lines indicate where the noise-removal framework is introduced.

algorithm. Then, we “subtract” the mean out from the observed stimulus-dependent data. Obviously, for random variables X, Y in vector spaces one cannot assume that $\tilde{X} = X + Y - \bar{Y}$ (\bar{Y} denotes the mean of Y) is a noise-reduced “version” of $X + Y$. However, in the space of spike trains we managed to establish this procedure, utilizing the warping matchings on the GVP mean. The procedure of obtaining $\tilde{X} = X \oplus Y \ominus \bar{Y}$ indeed gives a noise-reduced version \tilde{X} of a point pattern $X \oplus Y$. This approach is possible with definitions of the addition \oplus and the subtraction \ominus in the spike train space as follows:

Adding spike trains. We assume that the noise is additive and adding spike trains is achieved by union set operation. That is, let $X = (x_1, \dots, x_N)$ and $Y = (y_1, \dots, y_M)$ be two spike trains of length N and M , respectively. We define a spike train $Z = X \oplus Y$ as a spike train of length $N + M$ such that

$$Z = X \oplus Y = (\{x_1, \dots, x_N\} \cup \{y_1, \dots, y_M\}).$$

Subtracting spike trains. Defining the subtraction is more challenging, as it cannot follow directly from the set operations. This is due to the fact that it is unlikely to have coinciding spike times in two different spike trains. To perform the subtraction, we turn to the definition of the GVP metric and optimal warping between two spike trains [equation (1)]. We define the subtraction of a spike train Y from a spike train X as removing all spike positions from X that are matched with spikes in Y under the optimal warping γ . We say that a spike pair (x_i, y_j) is matched if $x_i = \gamma(y_j)$ for some pair (i, j) .

Formally, let $X = (x_1, \dots, x_N), Y = (y_1, \dots, y_M)$ be two spike trains and γ be the optimal warping between them according to the d_{GVP} metric. We define the subtraction of Y from X , noted by $Z = X \ominus Y$, as follows:

$$Z = X \ominus Y = (\{x_1, \dots, x_N\} \setminus \{x_i : x_i = \gamma(y_j) \text{ for some pair } (i, j)\}).$$

Once the \oplus and \ominus are established, we can describe the noise-removal method as follows: we “subtract” the $\text{mean}(Y)$ from the observed $X \oplus Y$

using the matching of the GVP metric and obtain a spike train $X \oplus Y \ominus \text{mean}(Y)$ by removing matched spikes. We at first use a simulation for illustration of both \oplus and \ominus operations in Section 3.2. The new method is then applied to a real experimental data set in Section 3.3.

3.2. Result for simulated data. To illustrate the noise-removal framework, we first generate 40 independent realizations $\{\mu_i\}_{i=1}^{40}$ of a homogeneous Poisson process on $[0, 2]$ with constant intensity $\alpha = 10$. These simulations represent the noise and are used to estimate the mean background noise $\hat{\mu}$ with the MAPC algorithm. The results are shown in Figure 4A.

Next we generate two sets of 20 independent spike trains, $\{X_i\}_{i=1}^{20}$ and $\{Y_i\}_{i=1}^{20}$, as realizations of an inhomogeneous Poisson processes (IPP) with intensity functions $\rho_X(t) = \exp(-(t - 1.5)^2)$ and $\rho_Y(t) = \exp(-(t - 0.5)^2)$, respectively. The generated spike trains are shown in Figure 4B. In our framework they correspond to the underlying true neuronal signals.

In the third step we obtain the equivalent of the “observed” data, by adding the previously generated noise for each generated μ_i to the corresponding spike trains X_i and Y_i . The combined results are shown in Figure 4C. In this case adding spike trains is understood in the set operations terms. We obtain spike trains following Poisson processes $X_i \oplus \mu_i \sim \text{IPP}(\rho_X + \alpha)$, $Y_i \oplus \mu_{i+20} \sim \text{IPP}(\rho_Y + \alpha)$.

The mean background noise spike train $\hat{\mu}$ is then subtracted out from each realization of the noised data set, according to the procedure described in Section 3.1. For each $i = 1, \dots, 20$, we obtain the noise removed spike trains: $X_i \oplus \mu_i \ominus \hat{\mu}$, $Y_i \oplus \mu_{i+20} \ominus \hat{\mu}$, shown in Figure 4D.

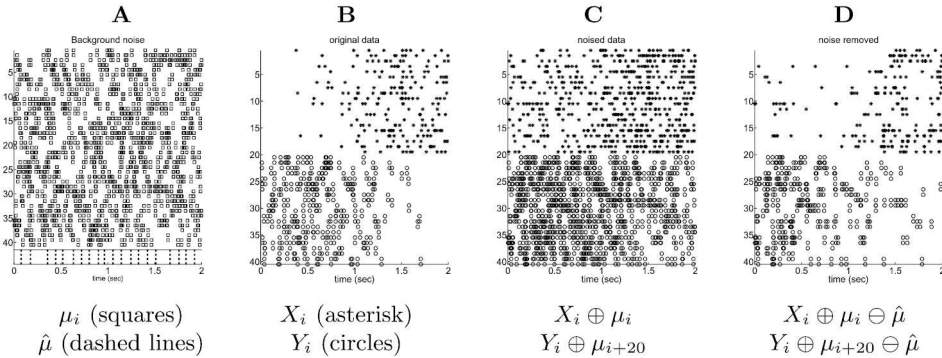


FIG. 4. Illustration of the noise addition and the noise removal with the use of the \oplus, \ominus operations. A: Background noise—40 spike trains generated from HPP(10); the mean background noise is presented with dashed lines in the bottom row. B: 2×20 spike trains from IPP(ρ_X) (asterisks) and IPP(ρ_Y) (circles), respectively. C: Sum of spike trains from A and B. D: Spike trains after the background noise removed.

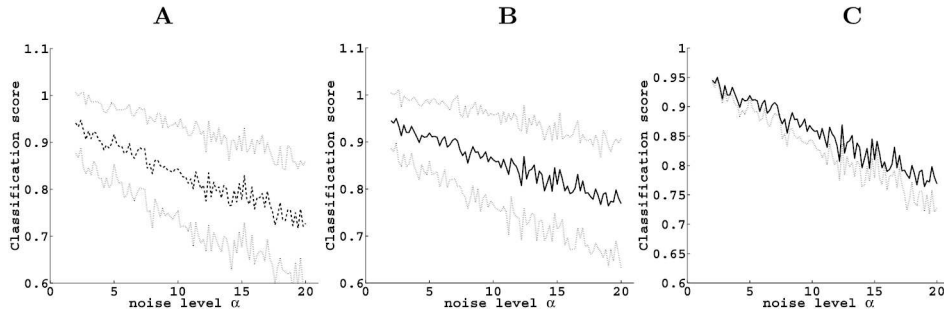


FIG. 5. *The noise-removal influence on classification performance with respect to increasing noise level α . A: The classification performance for the noisy data. The bold lines represent the average classification score among 50 simulations, the dotted lines indicate the standard deviation from the average classification score. B Same as A, but for the noise-removed data. C: Mean classification score curves from A (dashed line) and B (dotted line).*

We repeat this simulation procedure 50 times for each level of $\alpha \in [2, 20]$ and perform classification on the noisy data $X_i \oplus \mu_i, Y_i \oplus \mu_{i+20}$ as well as on the noise-removed: $X_i \oplus \mu_i \ominus \hat{\mu}, Y_i \oplus \mu_{i+20} \ominus \hat{\mu}$. The classification score is obtained by a standard leave-one-out cross-validation. We record the average score (the classification accuracy) with the standard deviation for each α level; the result is shown in Figure 5A, B. As anticipated with the increasing noise intensity α , the classification performance on each of the noisy and noise-reduced data sets declines. However, if we compare the two average classification scores presented in Figure 5C, we see that the noise-removal framework outperforms the classification on the noisy data once the noise intensity level α becomes not negligible. This result indicates that the proposed noise-removal procedure can help increase the contrast between different classes and result in an improvement in classification analysis. Next, we will examine this procedure on a real experimental data set.

3.3. Result in real data in gustatory system. Here we apply the noise-removal procedure to neural response in the gustatory system and test if the decoding (i.e., classification with respect to taste stimuli) can improve after the spontaneous activity is removed. The data consists of spike train recordings of rat geniculate ganglion neurons and was previously used in Wu et al. (2013). Briefly, adult male Sprague–Dawley rat’s geniculate ganglion tongue neurons were stimulated with 10 different solutions over a time period of 5 seconds: 0.1 M NaCl, 0.01 M citric acid (CA), 0.003, 0.01, 0.03, and 0.1 M acetic acid (AA), and each AA mixed with 0.1 M NaCl. Each stimulus was presented 2–4 times. Stimulus trials were divided into three time regions: a 5-second pre-stimulus period, a 5-second stimulus application period, and a

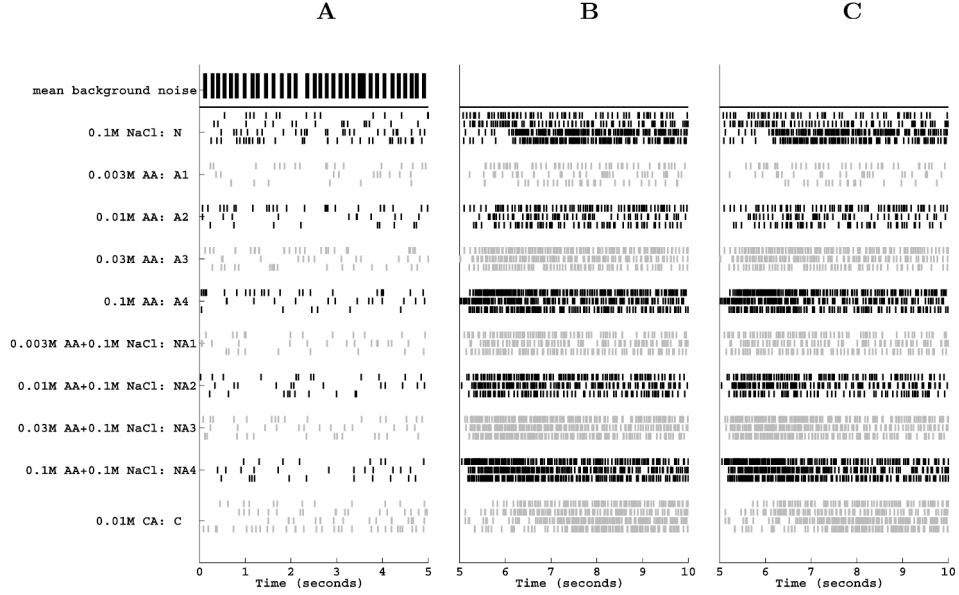


FIG. 6. An example of spike trains from Cell 10. Each group of 3 or 4 rows corresponds to a different type of stimuli applied. A: The 5-second pre-stimulus spike trains, whose mean spike train, calculated by the MAPC algorithm, is shown by the thick vertical bars on the top of the panel. B: The 5-second stimulus period. C: The same 5-second period of spike trains as in B, but with spontaneous activity subtracted out.

5-second post-stimulus period. During the first and third regions, a control solution of artificial saliva was applied. During the stimulus period, one of the 10 aforementioned solutions was applied. In this study we focus on classifying the given spike trains according to the 10 stimuli presented in each of 21 observed neurons. In Figure 6A, B we present the real data recordings in the first and second time regions from one example neuron.

The spike trains in the pre-stimulus 5-second period reflect spontaneous activity with artificial saliva applied. They are treated as “noise” data, in contrast to stimulus-dependent responses. We compute their mean spike train with the parameter $\lambda^2 = 0.001$ (a small value to get more spikes in the mean). The result is shown in the top row in Figure 6A. This mean properly summarizes spiking activity during the pre-stimulus period. In the next step, we subtract out this mean noise from the data during the stimulus period (spike trains between the 5th and 10th second). The noise-removed spike trains are shown in Figure 6C.

We can now compare the decoding performance using the observed stimulus-response data and the “noise-removed” data. To reliably evaluate classification scores, we take the approach of leave-one-out cross-validation. In both cases of the observed data and the noise-removed data, the class

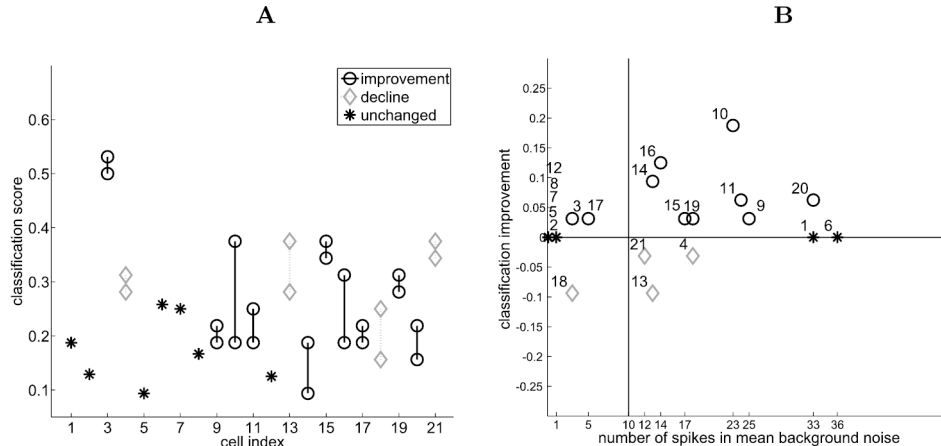


FIG. 7. The result of the noise-removal procedure applied to each of the recorded 21 cells. The marker coding is the same for both panels and indicates the influence of the noise-removal approach on the classification score: black circles—increase, grey diamonds—decrease, black asterisks—unchanged. A. Raw classification scores for each cell in each condition. B. Same result as in A, but in terms of classification score increase with respect to mean noise size. The vertical black line corresponds to the noise size cutoff of 10 spikes.

is assigned according to the nearest neighbor’s class under the d_{GVP} metric. In this classification analysis, we use $\lambda^2 = 225$, a relatively larger value to emphasize the importance of both matching term and penalty term in equation (1).

The comparison on the classification accuracy is shown in Figure 7A. In 10 out of 21 cells the classification was improved after the noise-removal procedure and in only 4 cells the classification was hindered. Classification in 7 cells remained unchanged after noise removal, which seems to be quite significant. To explain this issue, we have investigated the size of the mean background noise and its influence on increase in classification performance. It turned out, as seen in Figure 7B, that in 5 out of these 7 unchanged cells, the pre-stimulus spiking is negligible (the estimated mean spike train has 0 or 1 spike). In those cases, obviously, subtracting out the mean noise spike train will bare minimum influence.

The remaining two cases are associated with the opposite problem of the noise size—the number of spikes in the pre-stimulus period is comparable or greater than the number of spikes in the stimulation period. When such mean noise is subtracted out, it also can take away relevant information, thus it may not improve the decoding. Those noise size issues are consistent with common intuition behind the noise removal. However, it is worth noting that the size of the estimated mean background noise can be controlled in our new framework, by adjusting the penalty parameter λ (Section 2.4). More investigation will be conducted on the selection of λ in our future work.

When focusing on cells that have significant noise influence in their spiking pattern (at least 10 spikes in the estimated mean noise spike train), we see that in the majority of cases (8 out of 13) the noise removal has improved the classification score (Figure 7B). In extreme cases we obtain up to 20% improvement in the decoding performance. (Note that with 10 different stimuli, a random guess results in 10% average accuracy.) Only 3 out of the 13 cells indicate loss of information and 2 are not influenced by noise removal.

In summary, we find that our notion of mean background noise for spike train data is in agreement with the common understanding of the additive noise for the majority of recorded neurons. Moreover, the proposed noise-removal framework effectively improves neural decoding, provided that the pre-stimulus spiking has a high enough intensity.

4. Discussion. In this article we propose a new framework for defining the mean of a set of spike trains and the deviation from the mean. We provide an efficient algorithm for computing the mean spike train and prove the convergence of the method. The framework is based on the d_{GVP} metric [Dubbs, Seiler and Magnasco (2010)] which resembles the Euclidean distance. This concept gives an intuitive sample mean point pattern, in which the spike positions in the mean are averaged among matched spikes in a set of all spike trains.

Our summary statistics provide the basis for inference on point pattern data and in this article we utilize it to develop a mean-based noise-removal approach. We show that our procedure improves the classification score for simulated inhomogeneous Poisson point process data with various nonnegligible noise levels. We have also applied the new tools to a neural decoding problem in a rat's gustatory system. It is found that the mean point pattern approach and the noise-removal framework significantly improved the neural decoding among the set of 21 neurons.

In the noise-removal framework, we have defined the operations of addition and subtraction between spike trains with the use of the matching component of the GVP metric. We, however, note that those operations do not satisfy the law of associativity. For more advanced analysis, it is desirable to establish an algebraic structure on the space of point patterns. Thus, refining those approaches will be pursued in the further work.

Once the algebraic structure is established, statistical models can be built and regression analysis can be performed. With this setting and the already developed mean and the deviation from the mean approaches, we expect to develop classical statistical inferences such as hypothesis tests, confidence intervals/regions, FANOVA (functional ANOVA), FPCA (functional PCA), and regressions on functional data [Ramsay and Silverman (2005), Valderama (2007)]. All these tools are expected to provide a new methodology

for more effective analysis and modeling of neural spike trains or any point pattern data in general.

APPENDIX

THEOREM 1 (Convergence of the MAPC algorithm). *Denote the estimated mean in the m th iteration of the MAPC-algorithm as $S^{(m)}$. Then the sum of squared distances $\sum_{k=1}^K d_{\text{GVP}}(S^k, S^{(m)})^2$ decreases iteratively. That is,*

$$\sum_{k=1}^K d_{\text{GVP}}(S^k, S^{(m+1)})^2 \leq \sum_{k=1}^K d_{\text{GVP}}(S^k, S^{(m)})^2.$$

PROOF. The proof will go through steps 2–6 of the algorithm—in each step we will show that the overall distance to the proposed mean $S^{(m)} = (s_1^{(m)}, \dots, s_n^{(m)})$ is nonincreasing:

1. *Matching:* In the m th iteration, we find the optimal matching γ^k from $S^{(m)}$ to S^k for each $k \in \{1, \dots, K\}$. Having those, we can write

$$\begin{aligned} & \sum_{k=1}^K d_{\text{GVP}}(S^k, S^{(m)})^2 \\ &= \sum_{k=1}^K E_{\text{OR}}(S^k, \gamma^k(S^{(m)})) + \lambda^2 \sum_{k=1}^K \sum_{\{i,j:s_i^k=\gamma^k(s_j^{(m)})\}} (s_i^k - s_j^{(m)})^2. \end{aligned}$$

2. *Adjusting:* By definition, we update $S^{(m)}$ to $\tilde{S}^{(m)} = (\tilde{s}_1^{(m)}, \dots, \tilde{s}_n^{(m)}) = \frac{1}{K} \sum_{k=1}^K R_k$, where $R_k = (r_1^k, \dots, r_n^k)$ with

$$r_j^k = \begin{cases} s_i^k, & \text{if } \exists i \in \{1, \dots, n_k\}, \text{ s.t. } \gamma^k(s_j^{(m)}) = s_i^k, \\ s_j^{(m)}, & \text{otherwise} \end{cases}$$

$$k = 1, \dots, K, j = 1, \dots, n.$$

Hence, $\sum_{k=1}^K \sum_{\{i,j:s_i^k=\gamma^k(s_j^{(m)})\}} (s_i^k - s_j^{(m)})^2 = \sum_{k=1}^K \sum_{j=1}^n (r_j^k - s_j^{(m)})^2 \geq \sum_{k=1}^K \sum_{j=1}^n (r_j^k - \tilde{s}_j^{(m)})^2$.

Let γ be the piecewise linear warping function from $S^{(m)}$ to $\tilde{S}^{(m)}$, that is, $\tilde{S}^{(m)} = \gamma(S^{(m)})$. Then

$$\sum_{k=1}^K d_{\text{GVP}}(S^k, S^{(m)})^2$$

$$\begin{aligned}
 &\geq \sum_{k=1}^K E_{\text{OR}}(S^k, \gamma^k(S^{(m)})) + \lambda^2 \sum_{k=1}^K \sum_{j=1}^n (r_j^k - \tilde{s}_j^{(m)})^2 \\
 &\geq \sum_{k=1}^K E_{\text{OR}}(S^k, \gamma^k(S^{(m)})) + \lambda^2 \sum_{k=1}^K \sum_{\{i,j:s_i^k=\gamma^k(s_j^{(m)})\}} (s_i^k - \tilde{s}_j^{(m)})^2 \\
 &= \sum_{k=1}^K E_{\text{OR}}(S^k, \gamma^k \circ \gamma^{-1}(\tilde{S}^{(m)})) + \lambda^2 \sum_{k=1}^K \sum_{\{i,j:s_i^k=\gamma^k \circ \gamma^{-1}(\tilde{s}_j^{(m)})\}} (s_i^k - \tilde{s}_j^{(m)})^2 \\
 &\geq \sum_{k=1}^K d_{\text{GVP}}(S^k, \tilde{S}^{(m)})^2.
 \end{aligned}$$

3. *Pruning*: $\tilde{S}^{*(m)} = \{s_j \in \tilde{S}^{(m)} \mid \sum_{k=1}^K 1_{s_j \in \gamma^k(S^k)} \geq K/2\}$ is a subset of $\tilde{S}^{(m)}$ in which all spikes appear in $\{\gamma^k(S^k)\}_{k=1}^K$ at least $K/2$ times. Based on the result in the Adjusting step, we have $\sum_{k=1}^K d_{\text{GVP}}(S^k, S^{(m)})^2 \geq \sum_{k=1}^K E_{\text{OR}}(S^k, \gamma^k \circ \gamma^{-1}(\tilde{S}^{(m)})) + \lambda^2 \sum_{k=1}^K \sum_{\{i,j:s_i^k=\gamma^k \circ \gamma^{-1}(\tilde{s}_j^{(m)})\}} (s_i^k - \tilde{s}_j^{(m)})^2$. Using the basic rule of the Exclusive OR, it is easy to find that

$$\sum_{k=1}^K E_{\text{OR}}(S^k, \gamma^k \circ \gamma^{-1}(\tilde{S}^{*(m)})) \leq \sum_{k=1}^K E_{\text{OR}}(S^k, \gamma^k \circ \gamma^{-1}(\tilde{S}^{(m)})).$$

Let $\tilde{S}^{*(m)} = (s_1^{*(m)}, \dots, s_{n^*}^{*(m)})$, where n^* denotes the number of spikes in $\tilde{S}^{*(m)}$. Then,

$$\begin{aligned}
 &\sum_{k=1}^K d_{\text{GVP}}(S^k, S^{(m)})^2 \\
 &\geq \sum_{k=1}^K E_{\text{OR}}(S^k, \gamma^k \circ \gamma^{-1}(\tilde{S}^{*(m)})) + \lambda^2 \sum_{k=1}^K \sum_{\{i,j:s_i^k=\gamma^k \circ \gamma^{-1}(\tilde{s}_j^{*(m)})\}} (s_i^k - \tilde{s}_j^{*(m)})^2 \\
 &\geq \sum_{k=1}^K d_{\text{GVP}}(S^k, \tilde{S}^{*(m)})^2.
 \end{aligned}$$

4. *Checking*: Finally, we perform the checking step to avoid the possible local minima in the pruning process. In the test if a spike can be removed from $\tilde{S}^{*(m)}$, we let $\hat{S}^{*(m)}$ be $\tilde{S}^{*(m)}$ except one spike with a minimal number

of appearances. Then update the mean spike train as

$$S^{**}(m) = \begin{cases} \hat{S}^{*(m)}, & \text{if } \sum_{k=1}^K d_{\text{GVP}}(S^k, \hat{S}^{*(m)})^2 < \sum_{k=1}^K d_{\text{GVP}}(S^k, \tilde{S}^{*(m)})^2, \\ \tilde{S}^{*(m)}, & \text{otherwise.} \end{cases}$$

It is easy to verify that $\sum_{k=1}^N d_{\text{GVP}}(S^k, S^{(m)})^2 \geq \sum_{k=1}^N d_{\text{GVP}}(S^k, S^{**}(m))^2$. In the test if a spike can be added to $\tilde{S}^{**}(m)$, we let $\hat{S}^{**}(m)$ be $S^{**}(m)$ with one spike inserted at random within $[0, T]$. Then update the mean spike train as

$$S^{***}(m) = \begin{cases} \hat{S}^{**}(m), & \text{if } \sum_{k=1}^K d_{\text{GVP}}(S^k, \hat{S}^{**}(m))^2 < \sum_{k=1}^K d_{\text{GVP}}(S^k, S^{**}(m))^2, \\ \tilde{S}^{**}(m), & \text{otherwise.} \end{cases}$$

It is easy to see that $\sum_{k=1}^K d_{\text{GVP}}(S^k, S^{(m)})^2 \geq \sum_{k=1}^K d_{\text{GVP}}(S^k, S^{***}(m))^2$. Using step 6, the mean at the $(m+1)$ th iteration is $S^{(m+1)} = S^{***}(m)$. Hence,

$$\sum_{k=1}^K d_{\text{GVP}}(S^k, S^{(m+1)})^2 \leq \sum_{k=1}^K d_{\text{GVP}}(S^k, S^{(m)})^2. \quad \square$$

REFERENCES

- ARONOV, D. and VICTOR, J. D. (2004). Non-Euclidean properties of spike train metric spaces. *Phys. Rev. E* (3) **69** 061905, 9. [MR2096492](#)
- ARONOV, D., REICH, D. S., MECHLER, F. and VICTOR, J. D. (2003). Neural coding of spatial phase in V1 of the macaque monkey. *J. Neurophysiol.* **89** 3304–3327.
- BOX, G. E. P., HUNTER, W. G. and HUNTER, J. S. (1978). *Statistics for Experimenters: An Introduction to Design, Data Analysis, and Model Building*. Wiley, New York. [MR0483116](#)
- BREZA, J. M., NIKONOV, A. A. and CONTRERAS, R. J. (2010). Response latency to lingual taste stimulation distinguishes neuron types within the geniculate ganglion. *J. Neurophysiol.* **103** 1771–1784.
- BROWN, E. N., BARBIERI, R., VENTURA, V., KASS, R. E. and FRANK, L. M. (2002). The time-rescaling theorem and its application to neural spike train data analysis. *Neural Comput.* **14** 325–346.
- DIEZ, D. M., SCHOENBERG, F. P. and WOODY, C. D. (2012). Algorithms for computing spike time distance and point process prototypes with application to feline neuronal responses to acoustic stimuli. *J. Neurosci. Methods* **203** 186–192.
- DI LORENZO, P. M., CHEN, J. and VICTOR, J. D. (2009). Quality time: Representation of a multidimensional sensory domain through temporal decoding. *J. Neurosci.* **29** 9227–9238.
- DUBBS, A. J., SEILER, B. A. and MAGNASCO, M. O. (2010). A fast L^p spike alignment metric. *Neural Comput.* **22** 2785–2808. [MR2760538](#)
- HOUGHTON, C. (2009). Studying spike trains using a van Rossum metric with a synapse-like filter. *J. Comput. Neurosci.* **26** 149–155. [MR2481024](#)

- HOUGHTON, C. and SEN, K. (2008). A new multineuron spike train metric. *Neural Comput.* **20** 1495–1511. [MR2410365](#)
- HUNTER, J. D. and MILTON, J. G. (2003). Amplitude and frequency dependence of spike timing: Implications for dynamic regulation. *J. Neurophysiol.* **90** 387–394.
- JULIENNE, H. and HOUGHTON, C. (2013). A simple algorithm for averaging spike trains. *J. Math. Neurosci. (JMN)* **3** 1–14.
- KARCHER, H. (1977). Riemannian center of mass and mollifier smoothing. *Comm. Pure Appl. Math.* **30** 509–541. [MR0442975](#)
- KASS, R. E. and VENTURA, V. (2001). A spike-train probability model. *Neural Comput.* **13** 1713–1720.
- KASS, R. E., VENTURA, V. and BROWN, E. N. (2005). Statistical issues in the analysis of neuronal data. *J. Neurophysiol.* **94** 8–25.
- KREUZ, T., HAAS, J. S., MORELLI, A., ABARBANEL, H. D. I. and POLITI, A. (2007). Measuring spike train synchrony. *J. Neurosci. Methods* **165** 151–161.
- LAWHERN, V., NIKONOV, A. A., WU, W. and CONTRERAS, R. J. (2011). Spike rate and spike timing contributions to coding taste quality information in rat periphery. *Frontiers in Integrative Neuroscience* **5** 1–14.
- LIM, D. and CAPRANICA, R. R. (1994). Measurement of temporal regularity of spike train responses in auditory nerve fibers of the green treefrog. *J. Neurosci. Methods* **52** 203–213.
- MACLEOD, K., BÄCKER, A. and LAURENT, G. (1998). Who reads temporal information contained across synchronized and oscillatory spike trains? *Nature* **395** 693–698.
- PAIVA, A. R. C., PARK, I. and PRÍNCIPE, J. C. (2009). A reproducing kernel Hilbert space framework for spike train signal processing. *Neural Comput.* **21** 424–449. [MR2477866](#)
- QUIAN QUIROGA, R., KREUZ, T. and GRASSBERGER, P. (2002). Event synchronization: A simple and fast method to measure synchronicity and time delay patterns. *Phys. Rev. E (3)* **66** 041904, 9. [MR1935193](#)
- RAMSAY, J. O. and SILVERMAN, B. W. (2005). *Functional Data Analysis*, 2nd ed. Springer, New York. [MR2168993](#)
- RIEKE, F., WARLAND, D., DE RUYTER VAN STEVENINCK, R. and BIALEK, W. (1999). *Spikes: Exploring the Neural Code*. MIT Press, Cambridge, MA. [MR1983010](#)
- SCHREIBER, S., FELLOUS, J. M., WHITMERC, D., TIESINGAA, P. and SEJNOWSKIB, T. J. (2003). A new correlation-based measure of spike timing reliability. *Neurocomputing* **52-54** 925–931.
- VALDERRAMA, M. J. (2007). An overview to modelling functional data. *Comput. Statist.* **22** 331–334. [MR2336339](#)
- VAN ROSSUM, M. C. W. (2001). A novel spike distance. *Neural Comput.* **13** 751–763.
- VICTOR, J. D., GOLDBERG, D. H. and GARDNER, D. (2007). Dynamic programming algorithms for comparing multineuronal spike trains via cost-based metrics and alignments. *J. Neurosci. Methods* **161** 351–360.
- VICTOR, J. D. and PURPURA, K. P. (1996). Nature and precision of temporal coding in visual cortex: A metric-space analysis. *J. Neurophysiol.* **76** 1310–1326.
- VICTOR, J. D. and PURPURA, K. P. (1997). Sensory coding in cortical neurons. *Ann. N.Y. Acad. Sci.* **835** 330–352.
- WU, W. and SRIVASTAVA, A. (2011). An information-geometric framework for statistical inferences in the neural spike train space. *J. Comput. Neurosci.* **31** 725–748. [MR2864743](#)
- WU, W. and SRIVASTAVA, A. (2013). Estimating summary statistics in the spike-train space. *J. Comput. Neurosci.* **34** 391–410. [MR3061973](#)

WU, W., MAST, T. G., ZIEMBKO, C., BREZA, J. M. and CONTRERAS, R. J. (2013).
Statistical analysis and decoding of neural activity in the rodent geniculate ganglion
using a metric-based inference system. *PLoS ONE* **8** e65439.

S. WESOŁOWSKI
DEPARTMENT OF MATHEMATICS
FLORIDA STATE UNIVERSITY
TALLAHASSEE, FLORIDA 32306-4510
USA
E-MAIL: wesserg@gmail.com

R. J. CONTRERAS
DEPARTMENT OF PSYCHOLOGY
FLORIDA STATE UNIVERSITY
TALLAHASSEE, FLORIDA 32306-4301
USA
E-MAIL: contreras@psy.fsu.edu

W. WU
DEPARTMENT OF STATISTICS
FLORIDA STATE UNIVERSITY
TALLAHASSEE, FLORIDA 32306-4330
USA
E-MAIL: wwu@stat.fsu.edu